The DNA Minor Groove-alkylating Cyclopropylpyrroloindole Drugs Adozelesin and Bizelesin Induce Different DNA Damage Response Pathways in Human Colon Carcinoma HCT116 Cells[1]

Pei-rang Cao,[2] Mary M. McHugh,[2] Thomas Melendy, and Terry Beerman[3]

Department of Pharmacology and Therapeutics, Roswell Park Cancer Institute, Buffalo, New York 14263 [P-r. C., M. M. M., T. B.], and Department of Microbiology and the Witebsky Center for Microbial Pathogenesis and Immunology, University at Buffalo, State University of New York, School of Medicine and Biomedical Sciences, Buffalo, New York 14214 [T. M.]

Abstract

As members of the cyclopropylpyrroloindole family, adozelesin and bizelesin cause genomic DNA lesions by alkylating DNA. Adozelesin induces single-strand DNA lesions, whereas bizelesin induces both single-strand lesions and double-strand DNA cross-links. At equivalent cytotoxic concentrations, these agents caused different biological responses. Low adozelesin concentrations (*e.g.,* 0.5 nM) induced a transient S-phase block and cell cycle arrest in G_2-M, as well as increased induction of p53 and p21, whereas a high drug concentration (*e.g.,* 2.5 nM) caused apoptosis but no p21 induction. In contrast, both low and high bizelesin concentrations enhanced p53 and p21 induction and triggered G_2-M cell cycle arrest and eventual senescence without significant apoptotic cell death. However, in cells lacking p21, bizelesin, as well as adozelesin, triggered apoptosis, indicating that p21 was crucial to sustained bizelesin-induced G_2-M arrest. Thus, despite similar abilities to alkylate DNA, the chemotherapeutic agents adozelesin and bizelesin caused a decrease in HCT116 tumor cell proliferation by different pathways (*i.e.*, adozelesin induced apoptosis, and bizelesin induced senescence).

Introduction

Adozelesin and bizelesin (see Fig. 1), members of the CPI[4] family, alkylate in the minor groove of DNA at A-T rich regions (1). Adozelesin is a monofunctional CPI that alkylates at a single adenine, causing a single-strand DNA lesion (1). In contrast, bizelesin is a CPI dimer with two reactive chloromethyl moieties that can form DNA adducts with adenines in either one or both DNA strands, leading to single-strand DNA lesions or double-strand DNA cross-links, respectively (2).

When compared with other therapeutic agents that inhibit DNA synthesis by alkylating genomic DNA [*e.g.,* methylmethane sulfonate and cisplatin (3)], adozelesin and bizelesin are extraordinarily cytotoxic. They inhibit growth of a variety of murine and human tumor xenografts without the lethal hepatotoxicity caused by the parent compound CC-1065 (4, 5). Both adozelesin and bizelesin have undergone clinical trials (6).

Although they alkylate DNA with similar sequence preferences, the damage induced by adozelesin and bizelesin affects different biological responses. Bizelesin is more cytotoxic than adozelesin to both normal and tumor cells (7). Also, although both adozelesin and bizelesin block initiation of DNA synthesis in intact cells (8), adozelesin is severalfold more potent than bizelesin when DNA synthesis inhibition is measured either in intact cells or in a cell-free replication assay (8). Additionally, whereas adozelesin inhibits DNA replication by causing a decrease in functional RPA (9), bizelesin inhibits replication through induction of a replication inhibitor (8). The mechanisms involved in these differences are largely unknown.

Although the effect of bizelesin on the cell cycle has not been reported, adozelesin is known to trigger a transient slowing in cell cycle progression through S phase and arrest in G_2-M (4). Such a cell cycle response is observed with various types of DNA damage (10). Cells are transiently arrested in G_1, S, or G_2-M to allow time for DNA repair and to minimize the replication and segregation of damaged DNA (11). p53 plays an important role in the complex network of signals leading to arrest in different parts of the cell cycle (11). The G_1-S checkpoint is in part dependent on the p53-regulated transcription of p21, a potent inhibitor of the cyclin-CDK complex required for G_1-S transition (11). Likewise, p53 is involved in G_2-M arrest by its regulation of genes such as p21 and 14-3-3-σ (12), which allows activation of the Cdc2-cyclin B1 complex and reduced entry into mitosis (13).

In contrast to the G_1-S and G_2-M checkpoints, the S-phase checkpoint, which serves to prevent replication from occurring before repair is completed, is generally believed to be p53 independent (14). Whereas treatment during S-phase with DNA-damaging agents that specifically block DNA replication [*e.g.,* UV radiation (15) and hydroxyurea and aphidicolin (16)] leads to p53 accumulation and phosphorylation,

Received 1/21/03; revised 5/16/03; accepted 5/20/03.
The costs of publication of this article were defrayed in part by the payment of page charges. This article must therefore be hereby marked *advertisement* in accordance with 18 U.S.C. Section 1734 solely to indicate this fact.
[1] Supported by NIH Grants CA 77491 and CA 16056 (to T. A. B.) and NIH Grants CA89259 and AI01686 (to T. M.).
[2] Both authors contributed equally to this work.
[3] To whom requests for reprints should be addressed, at Department of Pharmacology and Therapeutics, Roswell Park Cancer Institute, Elm and Carlton Streets, Buffalo, NY 14263. Phone: (716) 845-3443; Fax: (716) 845-1575; E-mail: terry.beerman@roswellpark.org.
[4] The abbreviations used are: CPI, cyclopropylpyrroloindole; RPA, replication protein A; CDK, cyclin-dependent kinase; PARP, poly(ADP-ribose) polymerase; TUNEL, terminal deoxynucleotidyl transferase-mediated nick end labeling.

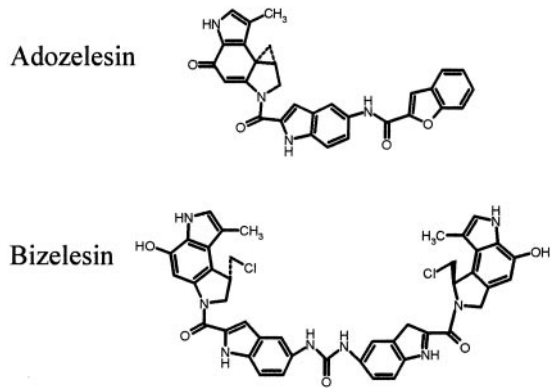

Fig. 1. Chemical structures of adozelesin and bizelesin.

induction of the p53 downstream targets p21 and HDM2 is not observed (15). The absence of p21 induction in S phase is due to an impaired transcriptional activity of p53 rather than to a general shutdown in cellular transcription (16). Thus, the ability of p53 to induce p21 differs with the phase of the cell cycle.

Other workers have shown that the consequences of DNA damage-induced cell cycle arrest may depend on the phase of the cycle in which arrest occurs. Apoptotic cells are reportedly arrested in S-phase, whereas senescence-like growth-arrested cells may show either G_1- or G_2-phase arrest (17). In this study, we compared the changes in cell cycle progression and initiation of cell death mechanisms induced by adozelesin and bizelesin. We examined whether adozelesin and bizelesin caused the p53 accumulation and p21 induction reported for other DNA-damaging agents. We showed that both the concentration and the type of CPI agent were important determinants of the phase of the cell cycle that was arrested and of whether this arrest led to decreased tumor cell proliferation via cell death or senescence.

Materials and Methods

Chemicals and Antibodies. Adozelesin and bizelesin were supplied by Pharmacia Corp. (Kalamazoo, MI), dissolved in DMSO, and stored at –20°C. Subsequent dilutions were made in growth medium. Propidium iodide and sodium cacodylate were obtained from Sigma Chemical Co. (St. Louis, MO). RNase and terminal deoxynucleoside triphosphate transferase were obtained from Roche Diagnostics, Co. (Indianapolis, IN). Monoclonal antibodies against human p53 (DO-1), p21 (SM-118), Bax, cyclin B1, PARP, and Bcl-2 were from PharMingen (San Diego, CA). Polyclonal antibody against human 14-3-3-σ was from Santa Cruz Biotechnology (Santa Cruz, CA). Polyclonal antibody against human p53 phosphorylated at serine 15 was obtained from Cell Signaling Technology (Beverly, MA). Anti-α-tubulin antibody was obtained from Sigma Chemical Co. All other chemicals were of reagent grade.

Cell Culture and Drug Treatment. HCT116 cells (clone 40-16) with wild-type p53 and p21-null HCT116 (clone 8054) cells were obtained from Prof. B. Vogelstein (Johns Hopkins University) and maintained in McCoy's 5a medium supplemented with 10% fetal bovine serum (Life Technologies, Inc., Grand Island, NY) in a 37°C incubator with 5% CO_2. Unless otherwise stated, 1×10^5 cells were seeded in 60-mm plates 48 h before drug treatment. Because 2–4 h is sufficient for site-specific alkylation of intracellular DNA by bizelesin and adozelesin (18) as well as by the parent CPI, CC1065 (19), cells were drug-treated for 4 h in all experiments. Cells treated with DMSO (the drug vehicle) served as controls. The DMSO concentration used was $<0.1\%$.

Clonogenic Assay. The assay used to determine drug effects on colony formation was described previously (20). Briefly, drug-treated HCT116 cells were collected by trypsinization, pelleted by centrifugation, resuspended in fresh medium, plated at 1×10^2 to 1×10^4 cells/35-mm plate, and cultured under normal growth conditions for 10 days. Cell colonies, defined as groups of >50 cells, were scored after staining with 0.5% methylene blue in 70% ethanol. Colony formation in drug-treated samples was expressed as a percentage of that in untreated control samples.

Flow Cytometry Analysis. Exponentially growing cells were treated with drug, rinsed with PBS, plated in drug-free medium, and cultured for the indicated times before harvesting. The cells were fixed in 70% ethanol, stained with propidium iodide solution (0.1% propidium iodide, 0.1% sodium citrate, 0.4% NP40 and 0.2 mg/ml RNase), and analyzed by flow cytometry on a FACscan instrument (Becton Dickinson, San Jose, CA) using Cell Quest software.

TUNEL Assay. Cells were grown on a coverslip to 70% confluence and then treated with drug for 4 h. After further incubation in drug-free medium for 48 h, cells were fixed in 1% formaldehyde for 10 min at room temperature. The TUNEL assay procedure was performed as described by Gorczyca *et al.* (21), with minor modifications. Briefly, cells were washed with 200 μl of reaction buffer containing 25 mM Tris-Cl (pH 6.6), 0.1 M sodium cacodylate, 1 mM $CoCl_2$, 0.1 mM DTT, and 0.5 mg/ml BSA. Cells were incubated in 50 μl of reaction buffer including 12.5 units of terminal deoxynucleoside triphosphate transferase and 0.5 nM FITC-dUTP for 45 min at room temperature. EDTA (0.2 M) was added to stop the reaction, and samples were placed on ice for 15 min. After washing with PBS containing Tween 20 (0.1%), coverslips were mounted on slides and analyzed by epimicroscopy with the appropriate filters.

Senescence-associated β-Galactosidase Activity Staining. After drug treatment, cells were incubated in drug-free medium for 10 days. Senescence-associated β-galactosidase activity was assayed as described by Dimri *et al.* (22), with minor modification. Briefly, cells were fixed in 3% formaldehyde in PBS for 25 min, washed three times with PBS, and then incubated at 37°C for 8 h with freshly prepared staining solution containing 1 mg/ml 5-bromo 4-chlororo-3-indolyl β-D-galactoside, 0.12 mM potassium ferricyanide, and 2 mM $MgCl_2$ in 100 mM phosphate buffer (pH 6.0). Cells were examined for β-galactosidase staining by epifluorescent microscopy.

Western Blotting. After drug treatment, cells were washed twice with PBS and lysed on ice for 15 min in 1 ml of

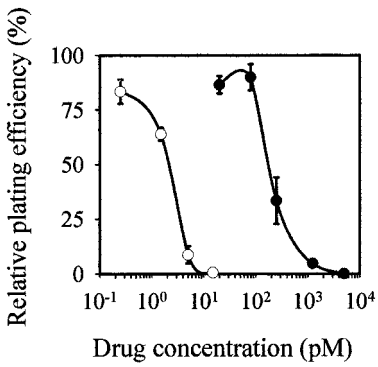

Fig. 2. Drug effects on HCT116 cell clonogenicity. HCT116 cells were treated with drug for 4 h and then serially diluted, replated, and grown for 10 days as described in "Materials and Methods." Relative plating efficiencies were calculated by dividing the plating efficiency observed with each drug treatment by the control plating efficiency. Adozelesin, ●; bizelesin, ○.

lysis buffer (400 mM NaCl, 0.1% NP40, 5 mM EDTA, 0.5 mM DTT, 1 mM phenylmethylsulfonyl fluoride, 0.1 mM sodium vanadate, 2 mM β-PP_i, 2 mM leupeptin, and 2 mM aprotinin). Whole cell lysates were subjected to centrifugation at 14,000 × *g* for 15 min. Protein concentrations were estimated using the Bradford assay kit (Bio-Rad Laboratories, Hercules, CA). Equal amounts of protein per lane were separated by electrophoresis on SDS-polyacrylamide gels and transferred to polyvinyldene difluoride membranes. The membranes were probed with the primary antibodies of interest followed by secondary antibodies conjugated with horseradish peroxidase, and the signal was visualized by enhanced chemiluminescence (ECL plus; Amersham Biosciences, Piscataway, NJ) and exposure to Kodak Biomax MS film (Eastman Kodak, Rochester, NY). The films were scanned, and the intensity of the protein bands was estimated using a densitometer and software from Molecular Dynamics (Sunnyvale, CA).

Results

Drug Effects on HCT116 Cell Clonogenicity. Changes in clonogenicity were used as a measure of adozelesin and bizelesin cytotoxicity in cultured human colorectal tumor HCT116 cells. Cells were treated with drug for 4 h, which allows sufficient time for CPI DNA alkylation reactions to occur (19). As shown in Fig. 2, both drugs were highly toxic, causing 50% inhibition of colony formation (IC_{50}) with 0.2 nM adozelesin and 2 pM bizelesin. These results were in agreement with studies by others in different cells lines (3, 23). In subsequent experiments, adozelesin and bizelesin were used at equivalent cytotoxic concentrations relative to their IC_{50} values. For example, 1× represented 0.2 nM adozelesin and 2 pM bizelesin. It is important to note that the 1× cytotoxic concentration, defined here as the concentration that causes a 50% decrease in colony formation, may or may not reflect actual killing of 50% of the cell population. For example, decreased colony formation also would be observed if cellular proliferation was inhibited (*e.g.,* if senescence is induced).

Effects of Adozelesin and Bizelesin on HCT116 Cell Cycle. The cell cycle effects of both adozelesin and bizelesin were examined using HCT116 cells. Cells were incubated with either drug for 4 h, followed by incubation for 24 or 48 h in drug-free medium. Changes in cell cycle progression are shown in Fig. 3*A*. Twenty-four h after treatment with 1× adozelesin (0.2 nM), 60–70% of cells were arrested in G_2-M. With 2.5× adozelesin (0.5 nM), cell cycle progression through S phase was also slowed, resulting in an accumulation of cells in S phase. At the highest adozelesin concentration [12.5× (2.5 nM)], most cells were blocked in G_0-G_1 with a substantial increase in the sub-G_0-G_1 fraction, suggestive of apoptosis (24). By contrast, 24 h after treatment with 1× (2 pM) to 12.5× (25 pM) bizelesin, 60–90% of cells were arrested in G_2-M. Fig. 3*B* is a graphical representation of the data from Fig. 3*A* showing the percentage of cells in the sub-G_0-G_1 fraction after incubation for 24 and 48 h after CPI treatment. A progressive increase in the sub-G_0-G_1 fraction to >20% of the cell population was observed with 1× to 12.5× adozelesin both 24 and 48 h posttreatment. However, this fraction accounted for <10% cells even 48 h after bizelesin treatment. No substantial increase in the sub-G_0-G_1 fraction was observed with bizelesin concentrations as high as 50× (100 pM) and 250× (0.5 nM; data not shown). These results suggest differing effects of equicytotoxic concentrations of adozelesin and bizelesin on HCT116 cell proliferation.

Extent of Apoptosis Induced in HCT116 Cells after Treatment with Adozelesin or Bizelesin. Because adozelesin, but not bizelesin, caused an increase in the sub-G_0-G_1 population, we examined whether either of these agents induced apoptosis. Cells were treated for 48 h with either adozelesin or bizelesin and stained with TUNEL reagents. In untreated (control) cells, no staining was observed (data not shown). However, a concentration-dependent increase in TUNEL staining was evident in adozelesin-treated samples (see Fig. 4*A*). At low adozelesin concentrations (1× and 2.5×), there were few stained cells in each field, indicating limited apoptosis. A large amount of positive staining was observed with 12.5× adozelesin, indicating extensive apoptosis. In contrast, little positive staining was observed in bizelesin-treated cells, and the signal intensity did not increase with the drug concentration.

Another molecular marker of apoptosis, degradation of PARP protein (25), was examined by Western blotting. As shown in Fig. 4*B*, reduced levels of PARP protein and the appearance of a PARP degradation product (molecular weight of 86,000) indicative of apoptosis were observed with the highest concentration (12.5×) of adozelesin but not bizelesin.

Even after prolonged incubation following treatment with bizelesin, no apoptosis was observed. For example, DNA ladder formation, an indication of apoptotic DNA fragmentation (26), was examined 4 days after drug treatment. Again, treatment with 12.5× adozelesin, but not bizelesin, caused DNA ladder formation (data not shown). Even after treatment with 250× (0.5 nM) bizelesin, DNA ladder formation was not observed.

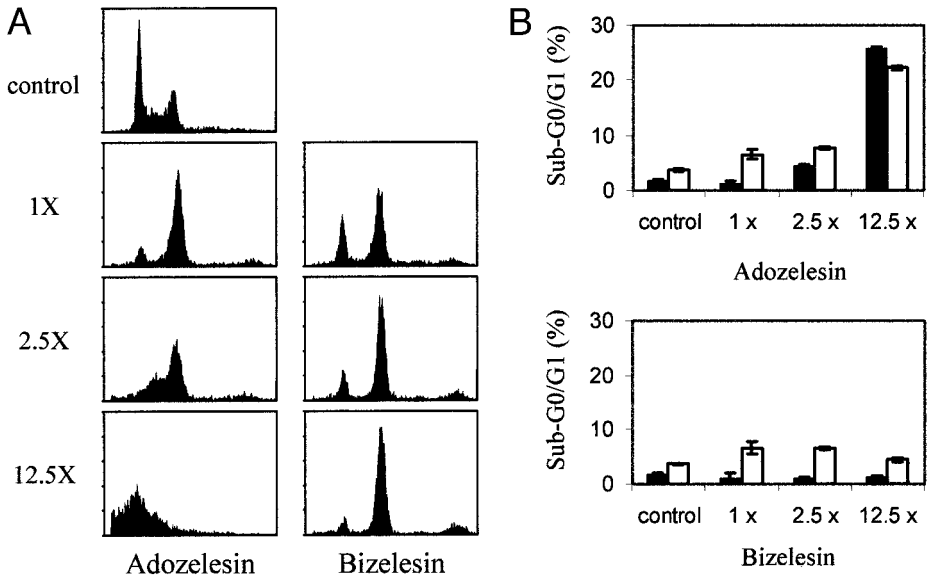

Fig. 3. Effects of adozelesin and bizelesin on the HCT116 cell cycle. HCT116 cells grown to 50% confluence were treated with drug for 4 h and further incubated in drug-free medium. The cells were collected, stained with propidium iodide, and analyzed by flow cytometry. A typical cell cycle distribution 24 h after treatment with adozelesin or bizelesin is shown in *A* and is representative of data from three individual experiments. The percentage total cells in the sub-G_0-G_1 population is shown in *B* and was calculated from the flow cytometry data. ■ and □ represent 24- and 48-h incubation after drug removal, respectively.

Bizelesin-induced Cell Cycle Arrest Leads to Senescence. Cell cycle arrest in G_2-M was observed 24 h post-treatment with >1× bizelesin and was sustained for at least 5 days (data not shown), indicating that the arrested cells could not reenter the cell cycle. Because bizelesin did not induce apoptosis, this decrease in cycling cells could be due to either nonapoptotic cell death or senescence. However, the hallmarks of nonapoptotic cell death, disruption of organelles and rupture of the plasma membrane (27), were not observed even 5 days after exposure to a high concentration (12.5×) bizelesin. Thus, whether these cells were senescent was investigated. Cells were treated with 2.5× bizelesin and washed to remove residual drug. After incubation in drug-free medium for 10 days, cells were stained for β-galactosidase activity, a biomarker for senescence (22). Fig. 5 shows untreated (*Control*) and bizelesin-treated cells. Only 1–5% of control cells stained positive for β-galactosidase. By contrast, the majority of the bizelesin-treated cells stained positively for β-galactosidase activity and showed a flat and enlarged morphology indicative of senescence. Because reduced growth factor levels in the medium after prolonged incubation times may contribute to positive staining, fresh medium was added to some samples after 5 days of incubation, and incubation was continued for an additional 5 days. However, providing the cells with fresh medium had no effect on senescence-positive staining (data not shown).

The Extent of p53-directed p21 Induction Differed with Adozelesin and Bizelesin Treatment. Because adozelesin and bizelesin induced differing cytotoxic responses in HCT116 cells, the molecular mechanisms of these responses were examined. Fig. 6*A* shows the effect of adozelesin and bizelesin on p53, a universal DNA damage sensor. When compared with the control levels, p53 protein was increased 24 h after treatment with either adozelesin or bizelesin. As drug concentrations were increased from 1× to 12.5×, p53 was increased 10–20-fold by adozelesin and 5–16-fold by bizelesin (Table 1). In response to DNA damage, phosphorylation of p53 at sites such as serine 15 and serine 20 leads to p53 protein stabilization, which activates p53-mediated transcription (11). Thus, we determined whether adozelesin or bizelesin treatment caused phosphorylation of p53 at serine 15. As shown in Fig. 6*A*, p53 phosphorylation at serine 15 was observed in both adozelesin- and bizelesin-treated cells but not in control cells.

p21 is a transcription target of p53 and is known to mediate cell cycle arrest (28). p21 was induced to different extents by adozelesin and bizelesin treatment (Fig. 6*A*). At 1×, adozelesin caused a 6-fold increase in p21 protein compared with control (Table 1). At 2.5×, no further increase in p21 was observed. However at 12.5×, despite high levels of p53 accumulation, minimal p21 was detected. In contrast, bizelesin concentrations of 1× to 12.5× effected a concentration-dependent increase in both p53 and p21. Thus, low concentrations (1× to 2.5×) of both agents that caused cells to accumulate in G_2 (see Fig. 3) also effected an increase in p21. With 1× to 12.5× bizelesin, both G_2 accumulation and enhanced levels of p21 were maintained. However, adozelesin levels that caused cells to accumulate in S phase (>2.5×) resulted in decreased levels of p21.

To determine whether the low levels of p21 protein observed with increasing adozelesin concentrations were due to a general decrease in protein synthesis, other proteins that are regulated in response to DNA damage were examined. Cyclin B1 varied similarly to p21 in response to adozelesin or bizelesin treatment (see Fig. 6*B*). With 1× adozelesin, cyclin B1 was increased, whereas 2.5× adozelesin resulted in cyclin B1 levels similar to those of the control. At 12.5× adozelesin, no cyclin B1 was detectable. All bizelesin concentrations induced an increase in cyclin B1 levels compared with control. Thus, CPI effects on cyclin B1 protein levels were similar to those described above for p21. By contrast, with increasing concentrations of adozelesin (as well as bizelesin), 14-3-3-σ, Bax, and *Bcl*II protein levels remained unchanged relative to control levels. Thus, changes in p21 (or

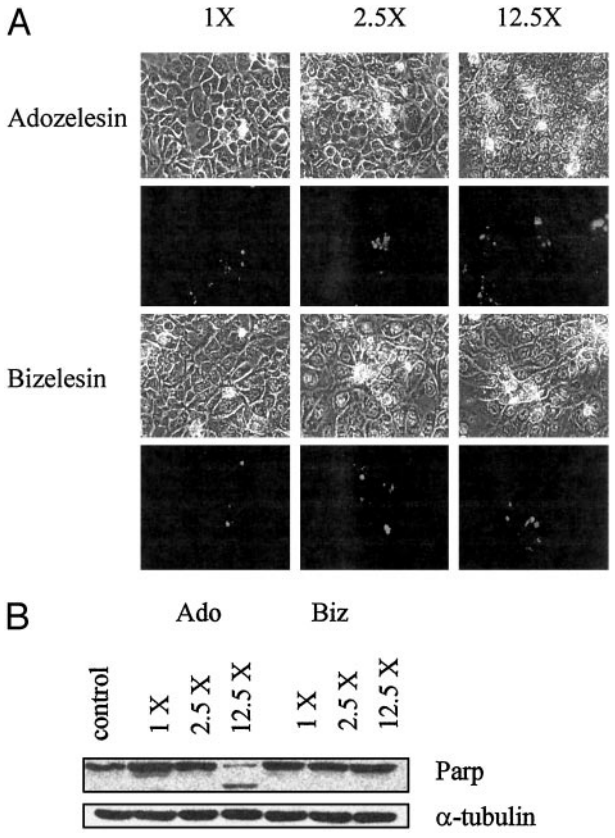

Fig. 4. Apoptotic response 48 h after adozelesin or bizelesin treatment. HCT116 cells grown on coverslips were treated with 1×, 2.5×, or 12.5× drug for 4 h and further incubated for 48 h in drug-free medium. After fixing with 1% formaldehyde, the cells were labeled using TUNEL reagents and examined at ×400 magnification using fluorescence epimicroscopy. In *A,* two panels are shown for each drug concentration. To directly compare the proportion of cells with a positive TUNEL reaction, fields with similar numbers of cells were chosen. The *top panel* is a phase-contrast image; the *bottom panel* is a fluorescent image. *B,* PARP detection. HCT116 cells were incubated for 24 h after drug removal, and cell lysates were subjected to SDS-PAGE and immunoblotted as described in "Materials and Methods." The antibody used was specific for human PARP protein. Tubulin was detected to assess whether equal amounts of proteins were loaded in all lanes.

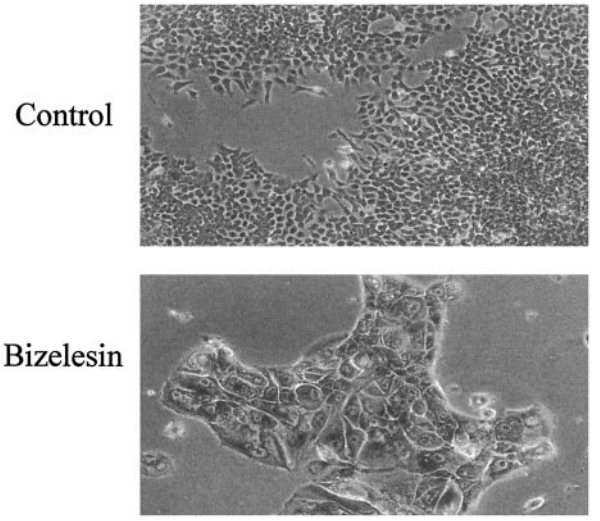

Fig. 5. HCT116 cell senescence 10 days after treatment with bizelesin. HCT116 cells were untreated (*Control*) or treated with 2.5× bizelesin for 4 h, and then further incubated in drug-free medium for 10 days. The cells were fixed, washed, and incubated with 5-bromo 4-chloro-3-indolyl β-D-galactoside at pH 6.0 for 8 h to detect β-galactosidase activity as described in "Materials and Methods." Control cells (*top panel*) were visualized at ×100 magnification to show the lack of β-galactosidase activity in a large field. The bizelesin-treated cells (*bottom panel*) were imaged by epimicroscopy at ×400 magnification.

cyclin B1) likely were not due to an adozelesin-directed decrease in overall protein synthesis.

Because reduced levels of p21 at high adozelesin concentrations do not result from a general decrease in cellular proteins, the transcriptional competence of induced p53 at various times after adozelesin treatment was examined. With 2.5× adozelesin, increased p53 and p21 protein accumulation was detected as early as 1 h, and accumulation continued to increase up to 24 h after drug treatment (Fig. 7). In contrast, 12.5× adozelesin induced maximal levels of p53 accumulation within 1 h and maintained this level for 24 h after treatment, whereas p21 levels were nearly undetectable over the entire time course. These results suggested that p53 induced by high concentrations of adozelesin was unable to stimulate p21 production, regardless of the posttreatment incubation time. By contrast, a gradual accumulation of both p53 and p21 proteins was observed between 1 and 24 h posttreatment with either low or high concentrations of bizelesin. Thus, p53 in bizelesin-treated cells remained transcriptionally competent.

Functional p21 Is Required for Maintenance of Bizelesin-induced G_2 Arrest. Because it appeared that p21 might be involved in stabilizing bizelesin-induced G_2 arrest, we examined whether G_2 arrest would be maintained in cells that failed to express p21. Fig. 8*A* shows cell cycle progression by p21-deficient HCT116 ($p21^{-/-}$) cells 24 and 48 h after a 4-h treatment with 1×, 2.5×, or 12.5× bizelesin. (Because bizelesin is 4-fold more cytotoxic to HCT116 $p21^{-/-}$ than to HCT116 cells, concentrations of 1×, 2.5×, and 12.5× in Fig. 8 represent 2.5, 6.25, and 25 pM bizelesin.) In contrast to the persistent G_2 arrest observed after bizelesin treatment of parent HCT116 cells, the effects of bizelesin on p21-deficient cells were concentration dependent. At low concentration (1×), G_2 arrest was noted, whereas increasing concentrations (*i.e.,* 2.5× and 12.5×) resulted in S-phase arrest and a pronounced accumulation of cells in the sub-G_0-G_1 fraction, indicative of DNA fragmentation (see cell cycle profile 48 h after treatment). Thus, effects of bizelesin on the cell cycle distribution of p21-deficient cells resembled the effects of adozelesin on p21 wild-type HCT116 cells (see Fig. 3*A*). Fig. 8*B* shows a progressive accumulation of cells in the sub-G_0-G_1 fraction 48 h after treatment with increasing concentrations (1× to 12.5×) of either adozelesin or bizelesin. With 12.5× of either drug, nearly 40% of the total cell population was shifted to the sub-G_0-G_1 fraction. The observation that maintenance of bizelesin-induced G_2-M arrest is not sustained in the absence of p21 suggests that p21 is required for directing bizelesin-treated cells toward G_2 arrest rather than apoptosis. In contrast, adozelesin-induced in-

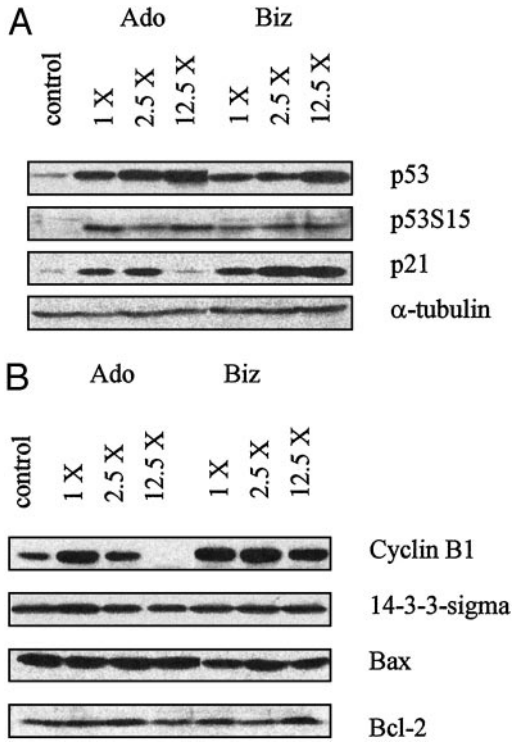

Fig. 6. Accumulation of p53, serine 15-phosphorylated p53, p21, cyclin B1, 14-3-3-σ, Bax, and Bcl-2 proteins in CPI-treated HCT116 cells. Cells were incubated with drug for 4 h, followed by 24 h in drug-free medium. Immunoblots were prepared as described in the Fig. 4 legend. CPI-induced effects on p53, p53 phosphorylated at serine 15, and p21 protein levels are shown in *A*, and effects on cyclin B1, 14-3-3-σ, Bax, and Bcl-2 protein levels are shown in *B*.

Table 1 Adozelesin- and bizelesin-induced changes in p53 and p21 protein levels in HCT116 cells

Cells were treated for 4 h and incubated for an additional 24 h in drug-free medium. Proteins were detected by Western blotting and quantitated as described in "Materials and Methods." p53 and p21 protein levels are expressed as fold increases over control. Data are from three individual experiments and are expressed (±SE).

	Drug dose[a]	Adozelesin	Bizelesin
p53	1×	10.1 ± 1.2	5.2 ± 3.6
	2.5×	15.7 ± 1.1	7.9 ± 0.3
	12.5×	19.6 ± 1.7	15.7 ± 4.5
p21	1×	5.7 ± 1.1	5.9 ± 0.2
	2.5×	6.6 ± 0.3	13.4 ± 2.5
	12.5×	0.9 ± 0.1	17.3 ± 3.5

[a] The drug concentration is expressed as a multiple of the IC_{50}.

creased accumulation in the sub-G_0-G_1 fraction was p21 independent because it was observed in both HCT116 $p21^{-/-}$ and the parent HCT116 cell line.

Discussion

This study showed dramatic differences in the effects of the monofunctional and bifunctional CPI alkylators adozelesin and bizelesin on HCT116 tumor cell proliferation. Low concentrations of adozelesin induced cell cycle arrest in G_2-M and slowed S-phase progression, whereas high concentrations caused apoptosis. Bizelesin induced a concentration-independent G_2-M arrest, and cells eventually became senescent. Increased p53 protein levels were observed with increasing concentrations of either drug. Likewise, p21 protein levels increased in cells arrested in G_2-M by either adozelesin or bizelesin. However, high concentrations of adozelesin, but not bizelesin, caused cells to accumulate in S phase and effected decreased p21 protein levels and eventual apoptosis. Thus, despite alkylating DNA through a common mechanism (18), these two agents evoke different tumor suppression pathways.

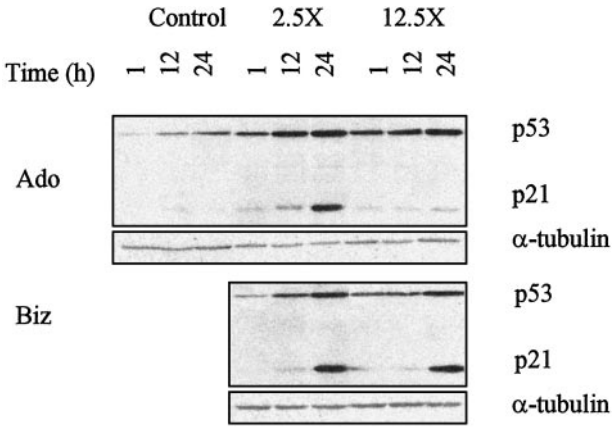

Fig. 7. Time course of accumulation of p53 and p21 proteins in drug-treated HCT116 cells. Cells were treated for 4 h with 0 (*Control*), 2.5×, or 12.5× adozelesin or bizelesin as indicated. Drug was replaced with fresh medium, and cells collected at the indicated times after drug removal were analyzed by Western blotting as described in the Fig. 4 legend.

In response to DNA damage, the cell cycle is arrested through checkpoint activation to allow cells time to repair damaged DNA or to die (11). For example, agents such as Adriamycin and cisplatin cause direct DNA damage and trigger cell cycle arrest in G_2-M (29, 30). With increasing DNA damage, p53 protein levels are increased, accompanied by phosphorylation at sites such as serine 15 (11). p53 induces p21 transcription (11), and this p53-dependent p21 induction is required to sustain G_2-M arrest in HCT116 cells (31). Other workers have shown that adozelesin causes p53 induction (9).

Low concentrations of either adozelesin or bizelesin caused G_2-M arrest and p53 accumulation with phosphorylation at serine 15 (see Fig. 6*A*) and an increase in p21 (see Table 1). p21 inhibits CDK, a component of the Cdc2-cyclin B1 complex, thus preventing entry into mitosis (13). Cells respond to CDK inhibition by increased levels of cyclin B1 (32). The observation that low concentrations of either adozelesin or bizelesin lead to an increase in cyclin B1, as well as an increase in p21, in concert with G_2-M arrest suggests that both agents caused the arrest through activation of the p53 and p21 pathways.

In addition to G_2-M arrest, increasing the adozelesin concentration to 2.5× caused an accumulation of cells in S phase, suggestive of replication inhibition. [An S-phase block was also observed 12 h after treatment with high concentration (12.5×) adozelesin.] The observation that this moderate

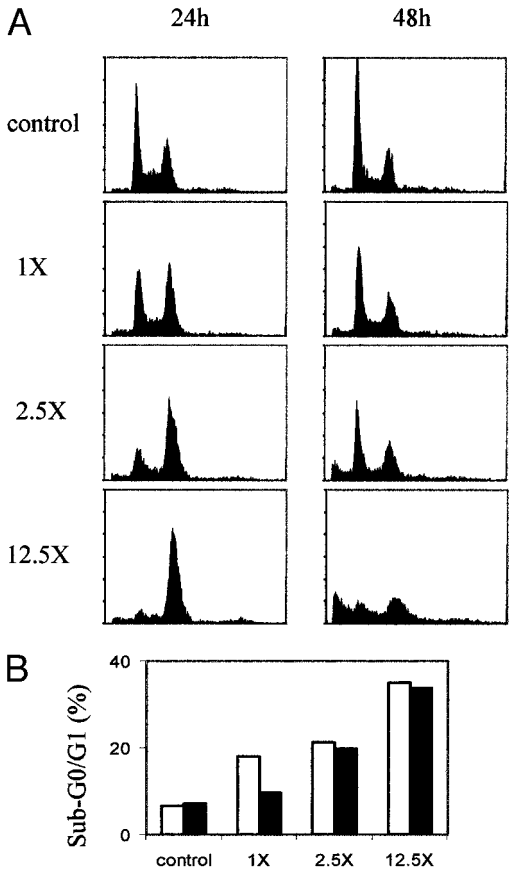

Fig. 8. Effects of adozelesin and bizelesin on p21-deficient HCT116 cell cycle distribution. After incubating HCT116 ($p21^{-/-}$) cells for 4 h with adozelesin or bizelesin, drug was replaced with fresh (drug-free) medium. Cells were further incubated for 24 and 48 h and analyzed by flow cytometry. *A,* fluorescence-activated cell-sorting profiles of cells 24 and 48 h after treatment with 1× to 12.5× bizelesin. *B,* accumulation of cells in sub-G_0-G_1 48 h after treatment with 1× to 12.5× adozelesin (□) or bizelesin (■).

concentration also caused an increased accumulation of p53 suggests that increased levels of p53 may play a role in replication inhibition. Previous studies from this laboratory showed in intact cells that adozelesin inhibited initiation of SV40 DNA synthesis (33). An *in vitro* replication assay correlated this inhibition with inactivation of the single-strand DNA-binding RPA (9). Other workers (34) have correlated inactivation of RPA by DNA-damaging agents such as UV with release of p53 from its association with a RPA-p53 complex. In addition, direct binding by p53 to DNA can inhibit replication (35). Thus, an increase in p53, whether due to its induction and stabilization or to its release by cellular components such as RPA, may directly inhibit DNA replication.

Recently, adozelesin was found to inhibit initiation of replication in human fibroblasts by decreasing Cdc6 binding to DNA during the early stages of programmed cell death (36). Other workers (37) have shown that activated T cells may become committed to apoptosis only after progressing into S phase. Thus, the S-phase checkpoint may be a crucial step in determining progression to apoptosis.

Whereas moderate concentrations of either adozelesin or bizelesin caused levels of p53 to increase, the increase with adozelesin was twice that of bizelesin (see Table 1). Other workers (17) have correlated the extent of p53 induction with the potential for a cell to undergo either apoptosis or senescence. After treatment of human fibroblasts with H_2O_2, both apoptotic and growth-arrested cells were observed. However, p53 protein levels in apoptotic cells were twice those in growth-arrested cells. Thus, higher induction of p53 was associated with apoptosis. Also, apoptotic cells were arrested primarily in S phase. The present study with adozelesin affirms this association of high levels of p53, S-phase arrest, and apoptosis. By contrast, H_2O_2-growth-arrested cells exhibited predominantly G_2-M-phase (as with bizelesin) or G1-phase distributions. Thus, the stage at which cells are arrested may impact whether cells progress to apoptosis or senescence.

Apoptosis can be regulated by the relative levels of Bax and members of the Bcl-2 family of apoptosis-promoting and apoptosis-inhibitory factors (38). After treatment with either adozelesin or bizelesin, Bax and Bcl-2 levels remained unchanged relative to untreated cells (see Fig. 6*B*). In addition, in HCT116 cells with two p53 knockout alleles, the extent of adozelesin-induced apoptosis was similar to that in wild-type HCT116 cells (data not shown). Thus, our data suggest that whereas p53 protein levels may increase with increasing adozelesin concentrations, the resultant apoptosis is independent of p53 or Bax pathways.

At the highest adozelesin concentration, high amounts of p53 accumulation and nearly undetectable levels of p21 were observed, indicating a failure to transcribe p21 (see Figs. 6 and 7). The absence of p21 is not likely due to protein degradation because no p21 fragmentation was observed. Other workers (16) have shown that HCT116 cells blocked in S phase induce high levels of p53 protein but not p53 transcriptional targets such as p21 and HDM-2, suggesting that p53 in S-phase-blocked cells is not fully active as a transcriptional factor. Furthermore, UV radiation reportedly induces a transcription-blocking DNA lesion that prevents p53 transactivation of p21 (39). Thus, it is possible that the transcriptional function of p53 is partly impaired when DNA synthesis is inhibited, or when DNA replication is stalled by DNA-damaging agents such as adozelesin.

Cyclin B1 levels in normal proliferating mammalian cells vary with the cell cycle, being low throughout G_1, increasing late in S, and becoming maximal at mitosis (40). Agents that alter cell cycle distribution might be expected to affect cyclin B1 protein levels. Cells blocked in G_2 by a low concentration of adozelesin or by 1× to 12.5× bizelesin exhibit high levels of cyclin B1 protein, likely because of the proportion of cells at the G_2-M boundary. However, 12.5× adozelesin caused cells to accumulate in S phase, possibly when cyclin B1 levels were already low. Thus, changes in cyclin B1 protein levels observed with increasing adozelesin concentrations may be due to altered cell cycle progression. Other workers (41) observed a similar effect on cyclin B1 protein levels after treatment of amnion cells with Adriamycin. As with adozelesin, a low concentration of Adriamycin caused G_2 arrest and accumulation of cyclin B1, whereas higher concentrations

caused S-phase arrest and cyclin B1 depletion. Thus, differences in cyclin B1 levels after CPI treatment may relate to the type of cell cycle block induced.

Whereas the effects of adozelesin on cell cycle progression were concentration dependent, bizelesin blocked cells in G_2-M regardless of the concentration, and cells eventually became senescent (see Fig. 5). Senescence induced by a variety of DNA-damaging agents in many mammalian cell lines, including HCT116 cells, is dependent on the presence of functional p21 (42). We observed p21 induction (Figs. 6*A* and 7) even 48 h after treatment with bizelesin (data not shown). By contrast, in isogenic $p21^{-/-}$ HCT116 cells (*i.e.*, cells lacking functional p21), bizelesin no longer caused senescence but rather cell death (see Fig. 8). Thus, senescence induced by bizelesin may be dependent, at least in part, on p21 induction.

DNA-damaging drugs can cause cell death or senescence, depending on the extent and the nature of DNA damage (*e.g.,* the amount of single- or double-strand lesions; Ref. 43). For example, cisplatin induces a variety of DNA adducts including inter- and intra-strand DNA cross-links and perturbs the cell cycle to different extents, depending on the amount of DNA damage (44). Low cisplatin concentrations may cause permanent cell cycle arrest (45), whereas higher concentrations can result in S-phase delay and apoptosis (46). In Chinese hamster fibroblast cells, low concentrations of the DNA strand scission agent bleomycin produce a moderate amount of single-strand breaks and cause G_2-M arrest, whereas higher concentrations cause an increase in DNA single-strand breaks, double-strand breaks, and apoptosis (43). In cultured human colorectal tumor HCT116 cells, induction of topoisomerase I-mediated DNA damage by low or high concentrations of camptothecin induces cell senescence or apoptosis, respectively (47). Thus, differing cytotoxic effects can be induced by a single drug, depending on the concentration at which it is administered.

Apoptosis may result from DNA damage exceeding a certain threshold (48). Whereas double-stranded bizelesin DNA adducts are more cytotoxic than single-strand lesions induced by adozelesin or by the parent CPI, CC-1065 [a 90% inhibition of cell growth requires only about 100 bizelesin lesions, compared with 10^4 CC-1065 lesions per cell (20)], adozelesin is reported to induce severalfold more lesions within discrete DNA regions (*i.e.*, the c-*myc* and apolipoprotein B genes) than does bizelesin (49). Thus, the different effects on tumor cell proliferation that we observed at equicytotoxic levels of adozelesin and bizelesin may be due to a higher total number of adozelesin-induced DNA lesions compared with bizelesin-induced DNA lesions, with higher lesion numbers leading to apoptosis, and lower amounts causing G_2-M cell cycle arrest and senescence.

In summary, we showed that at equitoxic concentrations, adozelesin and bizelesin induced different cellular responses. Adozelesin induced an S-phase slowdown preceding apoptosis that coincided with a decrease in p21 induction. Bizelesin induced cell cycle arrest in G_2-M through activation of the p53 and p21 pathways and cellular senescence. These differences may be due to the type of lesion and the extent of DNA damage: adozelesin may more extensively damage DNA and cause apoptosis; whereas the fewer, but more toxic, double-stranded bizelesin lesions lead to cell cycle arrest. Further work will examine how the extent of genomic DNA damage induced by these agents triggers cellular responses through either senescence or apoptosis.

Acknowledgments

We gratefully acknowledge Dr. Athena Lin for careful editing of the manuscript.

References

1. Li, L. H., Kelly, R. C., Warpehoski, M. A., McGovren, J. P., Gebhard, I., and DeKoning, T. F. Adozelesin, a selected lead among cyclopropylpyrroloindole analogs of the DNA-binding antibiotic, CC-1065. Investig. New Drugs, *9:* 137–148, 1991.

2. Lee, C. S., and Gibson, N. W. DNA interstrand cross-links induced by the cyclopropylpyrroloindole antitumor agent bizelesin are reversible upon exposure to alkali. Biochemistry, *32:* 9108–9114, 1993.

3. Bhuyan, B. K., Smith, K. S., Adams, E. G., Petzold, G. L., and McGovren, J. P. Lethality, DNA alkylation, and cell cycle effects of adozelesin (U-73975) on rodent and human cells. Cancer Res., *52:* 5687–5692, 1992.

4. Bhuyan, B. K., Smith, K. S., Adams, E. G., Wallace, T. L., Von Hoff, D. D., and Li, L. H. Adozelesin, a potent new alkylating agent: cell-killing kinetics and cell-cycle effects. Cancer Chemother. Pharmacol., *30:* 348–354, 1992.

5. Nguyen, H. N., Sevin, B. U., Averette, H., Perras, J., Ramos, R., and Donato, D. Spectrum of cell-cycle kinetics of alkylating agent adolezesin in gynecological cancer cell lines: correlation with drug-induced cytotoxicity. J. Cancer Res. Clin. Oncol., *118:* 515–522, 1992.

6. Carter, C. A., Waud, W. R., Li, L. H., DeKoning, T. F., McGovren, J. P., and Plowman, J. Preclinical antitumor activity of bizelesin in mice. Clin. Cancer Res., *2:* 1143–1149, 1996.

7. Lee, C. S., and Gibson, N. W. DNA damage and differential cytotoxicity produced in human carcinoma cells by CC-1065 analogues, U-73,975 and U-77,779. Cancer Res., *51:* 6586–6591, 1991.

8. McHugh, M. M., Kuo, S. R., Walsh-O'Beirne, M. H., Liu, J. S., Melendy, T., and Beerman, T. A. Bizelesin, a bifunctional cyclopropylpyrroloindole alkylating agent, inhibits simian virus 40 replication in trans by induction of an inhibitor. Biochemistry, *38:* 11508–11515, 1999.

9. Liu, J. S., Kuo, S. R., McHugh, M. M., Beerman, T. A., and Melendy, T. Adozelesin triggers DNA damage response pathways and arrests SV40 DNA replication through replication protein A inactivation. J. Biol. Chem., *275:* 1391–1397, 2000.

10. Kaufmann, W. K., and Kies, P. E. DNA signals for G_2 checkpoint response in diploid human fibroblasts. Mutat. Res., *400:* 153–167, 1998.

11. Lakin, N. D., and Jackson, S. P. Regulation of p53 in response to DNA damage. Oncogene, *18:* 7644–7655, 1999.

12. Zhou, B. B., and Elledge, S. J. The DNA damage response: putting checkpoints in perspective. Nature (Lond.), *408:* 433–439, 2000.

13. Elledge, S. J. Cell cycle checkpoints: preventing an identity crisis. Science (Wash. DC), *274:* 1664–1672, 1996.

14. Falck, J., Petrini, J. H., Williams, B. R., Lukas, J., and Bartek, J. The DNA damage-dependent intra-S phase checkpoint is regulated by parallel pathways. Nat. Genet., *30:* 290–294, 2002.

15. Chang, D., Chen, F., Zhang, F., McKay, B. C., and Ljungman, M. Dose-dependent effects of DNA-damaging agents on p53-mediated cell cycle arrest. Cell Growth Differ., *10:* 155–162, 1999.

16. Gottifredi, V., Shieh, S., Taya, Y., and Prives, C. From the cover: p53 accumulates but is functionally impaired when DNA synthesis is blocked. Proc. Natl. Acad. Sci. USA, *98:* 1036–1041, 2001.

17. Chen, Q. M., Liu, J., and Merrett, J. B. Apoptosis or senescence-like growth arrest: influence of cell-cycle position, p53, p21 and bax in H_2O_2 response of normal human fibroblasts. Biochem. J., *347:* 543–551, 2000.

18. Lee, C. S., Pfeifer, G. P., and Gibson, N. W. Mapping of DNA alkylation sites induced by adozelesin and bizelesin in human cells by ligation-

mediated polymerase chain reaction. Biochemistry, *33:* 6024–6030, 1994.

19. Zsido, T. J., Woynarowski, J. M., Baker, R. M., Gawron, L. S., and Beerman, T. A. Induction of heat-labile sites in DNA of mammalian cells by the antitumor alkylating drug CC-1065. Biochemistry, *30:* 3733–3738, 1991.

20. Woynarowski, J. M., McHugh, M. M., Gawron, L. S., and Beerman, T. A. Effects of bizelesin (U-77779), a bifunctional alkylating minor groove agent, on genomic and simian virus 40 DNA. Biochemistry, *34:* 13042–13050, 1995.

21. Gorczyca, W., Gong, J., and Darzynkiewicz, Z. Detection of DNA strand breaks in individual apoptotic cells by the *in situ* terminal deoxynucleotidyl transferase and nick translation assays. Cancer Res., *53:* 1945–1951, 1993.

22. Dimri, G. P., and Campisi, J. Molecular and cell biology of replicative senescence. Cold Spring Harbor Symp. Quant. Biol., *59:* 67–73, 1994.

23. Volpe, D. A., Tomaszewski, J. E., Parchment, R. E., Garg, A., Flora, K. P., Murphy, M. J., and Grieshaber, C. K. Myelotoxic effects of the bifunctional alkylating agent bizelesin on human, canine and murine myeloid progenitor cells. Cancer Chemother. Pharmacol., *39:* 143–149, 1996.

24. Tounekti, O., Belehradek, J., Jr., and Mir, L. M. Relationships between DNA fragmentation, chromatin condensation, and changes in flow cytometry profiles detected during apoptosis. Exp. Cell Res., *217:* 506–516, 1995.

25. Earnshaw, W. C., Martins, L. M., and Kaufmann, S. H. Mammalian caspases: structure, activation, substrates, and functions during apoptosis. Annu. Rev. Biochem., *68:* 383–424, 1999.

26. Fimia, G. M., Gottifredi, V., Passananti, C., and Maione, R. Double-stranded internucleosomal cleavage of apoptotic DNA is dependent on the degree of differentiation in muscle cells. J. Biol. Chem., *271:* 15575–15579, 1996.

27. Saraste, A. Morphologic criteria and detection of apoptosis. Herz, *24:* 189–195, 1999.

28. Chan, T. A., Hwang, P. M., Hermeking, H., Kinzler, K. W., and Vogelstein, B. Cooperative effects of genes controlling the G_2/M checkpoint. Genes Dev., *14:* 1584–1588, 2000.

29. Luo, Y., Rockow-Magnone, S. K., Kroeger, P. E., Frost, L., Chen, Z., Han, E. K., Ng, S. C., Simmer, R. L., and Giranda, V. L. Blocking Chk1 expression induces apoptosis and abrogates the G_2 checkpoint mechanism. Neoplasia, *3:* 411–419, 2001.

30. Bose, R. N. Biomolecular targets for platinum antitumor drugs. Mini Rev. Med. Chem., *2:* 103–111, 2002.

31. Bunz, F., Dutriaux, A., Lengauer, C., Waldman, T., Zhou, S., Brown, J. P., Sedivy, J. M., Kinzler, K. W., and Vogelstein, B. Requirement for p53 and p21 to sustain G_2 arrest after DNA damage. Science (Wash. DC), *282:* 1497–1501, 1998.

32. Wilson, D. W., Lame, M. W., Dunston, S. K., and Segall, H. J. DNA damage cell checkpoint activities are altered in monocrotaline pyrrole-induced cell cycle arrest in human pulmonary artery endothelial cells. Toxicol. Appl. Pharmacol., *166:* 69–80, 2000.

33. Cobuzzi, R. J., Jr., Burhans, W. C., and Beerman, T. A. Inhibition of initiation of simian virus 40 DNA replication in infected BSC-1 cells by the DNA alkylating drug adozelesin. J. Biol. Chem., *271:* 19852–19859, 1996.

34. Abramova, N. A., Russell, J., Botchan, M., and Li, R. Interaction between replication protein A and p53 is disrupted after UV damage in a DNA repair-dependent manner. Proc. Natl. Acad. Sci. USA, *94:* 7186–7191, 1997.

35. Cox, L. S., Hupp, T., Midgley, C. A., and Lane, D. P. A direct effect of activated human p53 on nuclear DNA replication. EMBO J., *14:* 2099–2105, 1995.

36. Blanchard, F., Rusiniak, M. E., Sharma, K., Sun, X., Todorov, I., Castellano, M. M., Gutierrez, C., Baumann, H., and Burhans, W. C. Targeted destruction of DNA replication protein cdc6 by cell death pathways in mammals and yeast. Mol. Biol. Cell, *13:* 1536–1549, 2002.

37. Radvanyi, L. G., Shi, Y., Mills, G. B., and Miller, R. G. Cell cycle progression out of G_1 sensitizes primary-cultured nontransformed T cells to TCR-mediated apoptosis. Cell. Immunol., *170:* 260–273, 1996.

38. Strasser, A., O'Connor, L., and Dixit, V. M. Apoptosis signaling. Annu. Rev. Biochem., *69:* 217–245, 2000.

39. McKay, B. C., Ljungman, M., and Rainbow, A. J. Persistent DNA damage induced by ultraviolet light inhibits p21waf1 and bax expression: implications for DNA repair, UV sensitivity and the induction of apoptosis. Oncogene, *17:* 545–555, 1998.

40. Lodish, H., Berk, A., Zipursky, L. S., Matsudaira, P., Baltimore, D., and Darnell, J. Molecular Cell Biology, 4th ed. New York: W. H. Freeman, 2000.

41. Minemoto, Y., Gannon, J., Masutani, M., Nakagama, H., Sasagawa, T., Inoue, M., Masamune, Y., and Yamashita, K. Characterization of adriamycin-induced G_2 arrest and its abrogation by caffeine in FL-amnion cells with or without p53. Exp. Cell Res., *262:* 37–48, 2001.

42. Itahana, K., Dimri, G., and Campisi, J. Regulation of cellular senescence by p53. Eur. J. Biochem., *268:* 2784–2791, 2001.

43. Tounekti, O., Pron, G., Belehradek, J., Jr., and Mir, L. M. Bleomycin, an apoptosis-mimetic drug that induces two types of cell death depending on the number of molecules internalized. Cancer Res., *53:* 5462–5469, 1993.

44. Gonzalez, V. M., Fuertes, M. A., Alonso, C., and Perez, J. M. Is cisplatin-induced cell death always produced by apoptosis? Mol. Pharmacol., *59:* 657–663, 2001.

45. Robles, S. J., Buehler, P. W., Negrusz, A., and Adami, G. R. Permanent cell cycle arrest in asynchronously proliferating normal human fibroblasts treated with doxorubicin or etoposide but not camptothecin. Biochem. Pharmacol., *58:* 675–685, 1999.

46. el Alaoui, S., Lawry, J., and Griffin, M. The cell cycle and induction of apoptosis in a hamster fibrosarcoma cell line treated with anti-cancer drugs: its importance to solid tumour chemotherapy. J. Neurooncol., *31:* 195–207, 1997.

47. Han, Z., Wei, W., Dunaway, S., Darnowski, J. W., Calabresi, P., Sedivy, J., Hendrickson, E. A., Balan, K. V., Pantazis, P., and Wyche, J. H. Role of p21 in apoptosis and senescence of human colon cancer cells treated with camptothecin. J. Biol. Chem., *277:* 17154–17160, 2002.

48. Fisher, D. E. Apoptosis in cancer therapy: crossing the threshold. Cell, *78:* 539–542, 1994.

49. Woynarowski, J. M., Napier, C., Trevino, A. V., and Arnett, B. Region-specific DNA damage by AT-specific DNA-reactive drugs is predicted by drug binding specificity. Biochemistry, *39:* 9917–9927, 2000.